

Overcoming erasure errors with multilevel systems

Sreraman Muralidharan¹, Chang-Ling Zou^{1,2,3}, Linshu Li², Jianming Wen², and Liang Jiang^{2*}

¹*Department of Electrical Engineering, Yale University, New Haven, CT 06511 USA*

²*Department of Applied Physics, Yale University, New Haven, CT 06511 USA and*

³*Key Laboratory of Quantum Information, University of Science and Technology of China, Hefei, 230026, People's Republic of China*

(Dated: June 14, 2022)

We propose to use efficient quantum error correcting codes with multilevel systems to protect encoded quantum information from erasure errors and efficient implementation to repetitively correct these errors. Our scheme makes use of quantum polynomial codes to encode quantum information and generalizes teleportation based error correction for multilevel systems to repetitively correct photon erasures and operation errors. We discuss the application of our scheme for one-way quantum repeaters and discuss their physical implementation using atom mediated multiqubit gates.

PACS numbers: 03.67.Dd, 03.67.Hk, 03.67.Pp.

Detectable erasure errors arise in various models of quantum computation in the form of photon erasures [1–4], qubit erasures [5] or leakage processes [6–8]. Protecting quantum information from erasure errors is an important challenge for realistic quantum computation and communication. One approach to correct erasure errors is heralded detection, which is often used in entanglement generation experiments to overcome photon erasures conditioned on certain photon click patterns [9–11]. However, heralded detection is a probabilistic scheme, which leads to additional overhead in temporal and physical resources [12]. Erasure errors can be corrected deterministically using error-correcting codes to encode the quantum information and by using error correction to correct them [13–16]. To achieve this, it is crucial to have efficient error correcting codes and robust implementation to correct erasure errors.

In general, any error correcting code can correct no more than 50% erasure error rates deterministically with one way communication owing to the no-cloning theorem [17]. Recently, there have been significant advances in searching for quantum codes that can correct up to 50% erasure error rates. Varnava *et. al.* [13] showed that by using tree-like cluster states for encoding, one can correct erasure error rates up to 50% bound for one way quantum computing. Stace and Barrett [14, 15] demonstrated that surface codes can also correct up to 50% erasure error rates. However, these codes often require large code size to enable the correction of a large fraction of erasure errors. In practice, it is desirable to have smaller size codes, which can achieve high success rates.

Quantum error correcting codes of higher-dimensional systems provide a new route to efficiently correct erasure errors. For example, quantum polynomial codes (QPyC) [18, 19] are an interesting class of CSS codes that were introduced in the context of quantum computation [18] and shown to be useful for quantum secret sharing [19], where one can encode a secret qudit into a $[[2k + 1, 1, k + 1]]_d$ quantum polynomial code of $2k + 1$ qudits (with prime

dimension $d \geq 2k + 1$) and distribute it among many parties, so that at least $(k + 1)$ of them should get together to reconstruct the secret. Moreover, QPyC is suitable for the correction of erasure errors up to a fraction of $k/(2k + 1) \rightarrow 50\%$ for a large k .

In this Letter, we first show the advantage of using QPyC for the correction of erasure errors over the qubit based encoding schemes for both small and large size codes. Then, we generalize teleportation based error correction (TEC) for the correction of erasure errors using QPyC. As an application, we consider using the QPyC for ultrafast one-way quantum repeater schemes, and demonstrate that optimized quantum repeaters that use QPyC for encoding can perform more efficiently than the previously known schemes [20, 21].

Error correction for erasure errors. To illustrate, how the error correction for erasure errors works, we first consider the four-qubit $[[4, 1, 2]]$ code that maps a qubit into the logical states [16, 22],

$$\begin{aligned} |0\rangle_L &= \frac{1}{2}(|00\rangle + |11\rangle)_{12}(|00\rangle + |11\rangle)_{34}, \\ |1\rangle_L &= \frac{1}{2}(|00\rangle - |11\rangle)_{12}(|00\rangle - |11\rangle)_{34}, \end{aligned} \quad (1)$$

where the subscripts 1-4 denote qubits 1-4. If one of the physical qubits undergoes an erasure error (say qubit 1), then the complementary qubit (qubit 2) is measured in the Z -basis and the measurement outcome can be used for reconstructing the encoded qubit [23]. We need at least *four* qubits to correct one erasure error [24]. In contrast, if we consider multilevel systems, we can actually correct an erasure error using a *three*-qutrit $[[3, 1, 2]]_3$ code that maps a qutrit into logical states [19],

$$\begin{aligned} |0\rangle_L &= \frac{1}{\sqrt{3}}(|000\rangle + |111\rangle + |222\rangle)_{123}, \\ |1\rangle_L &= \frac{1}{\sqrt{3}}(|012\rangle + |120\rangle + |201\rangle)_{123}, \\ |2\rangle_L &= \frac{1}{\sqrt{3}}(|021\rangle + |210\rangle + |102\rangle)_{123}, \end{aligned} \quad (2)$$

where, the subscripts 1-3 represent qutrits 1-3. If, a single qutrit is lost, it is possible to reconstruct the encoded qutrit by performing an addition modulo three operation on the remaining qutrits [23]. We compare the success probability P_{success} of the $[[3, 1, 2]]_3$ code with the $[[4, 1, 2]]$ code across different erasure error rates p_l in Fig. 1(a). It can be seen that the threshold for error correction for erasure errors is 50% for the $[[3, 1, 2]]_3$ code, while it is lower ($\approx 24\%$) for the $[[4, 1, 2]]$ code. This means that for $p_l < 50\%$ (24%) for the $[[3, 1, 2]]_3$ code ($[[4, 1, 2]]$ code), one can obtain a higher P_{success} by using quantum error correction instead of direct information transmission. The $[[3, 1, 2]]_3$ code outperforms the $[[4, 1, 2]]$ code for all erasure rates p_l . In principle, by concatenating the $[[3, 1, 2]]_3$ code, it is possible to suppress more erasure errors. However, to be resource efficient we will consider the following generalization of the $[[3, 1, 2]]_3$ code using multilevel systems.

Quantum Polynomial codes. The qutrit $[[3, 1, 2]]_3$ code can be generalized to d -level (d is a prime number) qudit system as $[[2k + 1, 1, k + 1]]_d$ codes, which encode one logical qudit into $2k + 1$ physical qudits and can correct up to k erasure errors [19]. The QPyC code is a CSS code which extends the classical $[2k + 1, 1, k + 1]$ polynomial code to the quantum scenarios with the encoded states [18],

$$|i\rangle_L = \sum_{c_{k-1}=i} |p_c(x_0), p_c(x_1), \dots, p_c(x_{m-1})\rangle, \quad (3)$$

where, x_0, x_1, \dots, x_{m-1} are distinct elements of \mathbf{F} , $p_c(x) = \sum_{j=0}^{k-1} c_j x^j$, $c_j \in \mathbf{F}^k$ and $\mathbf{F} = Z^d$. The success probability of decoding QPyC after it has undergone erasure errors is given by,

$$P_{\text{success}}^{\text{QPyC}} = \sum_{i=0}^k \binom{2k+1}{i} p_l^i (1-p_l)^{2k+1-i}. \quad (4)$$

In Fig. 1(b), we show that for a reasonable code size, it is possible to achieve substantially low failure rates $P_{\text{fail}} = 1 - P_{\text{success}}^{\text{QPyC}}$ even in the presence of high erasure rates p_l . It can be seen from Eq. (4) that at $p_l = 50\%$, $P_{\text{success}}^{\text{QPyC}} = 1/2$ independent of the code size. Further, note that the success probability of error correction has a phase transition with $k \rightarrow \infty$, $P_{\text{success}}^{\text{QPyC}} \rightarrow 1$ for $p_l \geq 50\%$ and $P_{\text{success}}^{\text{QPyC}} \rightarrow 0$ for $p_l < 50\%$. We obtain the critical exponent of phase transition by noting that for $k \rightarrow \infty$ [23],

$$P_{\text{success}}^{\text{QPyC}} \approx \frac{1}{2} - 2\sqrt{\frac{k}{\pi}} \left(p_l - \frac{1}{2}\right). \quad (5)$$

For a given $P_{\text{success}}^{\text{QPyC}}$, we need the QPyC with size

$$k \approx \frac{\pi}{4} \left(\frac{P_{\text{success}}^{\text{QPyC}} - \frac{1}{2}}{\frac{1}{2} - p_l} \right)^2, \quad (6)$$

yielding a critical exponent of 2.

We will now compare the performance of surface codes [25] with QPyC. Surface codes consists of a $D \times D$ square lattice with $2D^2$ qubits in total, where each qubit located on the edges of the square lattice. The logical operators X_L (Z_L) of the surface codes are given by the product of X (Z) operators along a non-trivial homological cycle connecting the boundaries [25]. The probability of measuring X_L and Z_L operators and decoding the surface code is essentially the success probabilities of bond percolation in the square lattice and its dual lattice. It is well known that the bond percolation threshold is 50% for a square lattice [26], meaning that as the distance of the lattice $D \rightarrow \infty$, $P_{\text{success}}^{\text{SC}} \rightarrow 1$ for $p_l < 50\%$ and $P_{\text{success}}^{\text{SC}} \rightarrow 0$ for $p_l > 50\%$. In Fig. 1(d) we study the success probabilities of surface codes with three different distances (3,7,12) and find that at $p_l = 1/2$, $P_{\text{success}}^{\text{SC}} \approx 0.30$, agreeing with the earlier numerical work on crossing probabilities on a square lattice [27]. In Fig. 1(c) we see that $P_{\text{success}}^{\text{QPyC}} = 0.5$ for all code sizes. Therefore, close to $p_l = 50\%$, QPyC of any code size always performs better than surface codes. Further, it can be seen in Fig. 1(d) that threshold for surface codes with $D = 3$ is about 37%, and it approaches 50% for larger code sizes, while the threshold of QPyC is 50% for all code sizes.

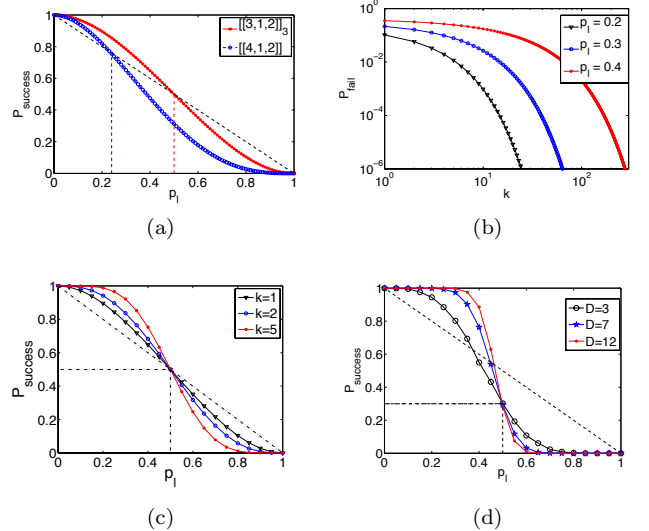


FIG. 1: (color online). a) A comparison between the success probabilities for the correction of one erasure error with $[[4, 1, 2]]$ and $[[3, 1, 2]]_3$ encoding. Dotted line indicates the success probability for no encoding and the point of intersection of the success probability with the dotted line indicates the threshold for error correction for erasure errors. (b) Effective erasure rate or the failure probability of QPyC for different code sizes. (c) Success probability of QPyC for different erasure rates. (d) Success probabilities of decoding surface codes with three different distances (3,7,12).

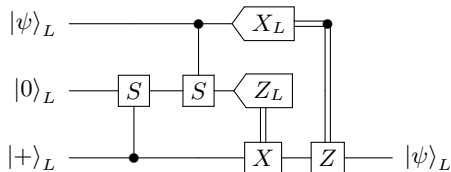


FIG. 2: TEC circuit for multilevel systems, where erasure and operation (X and Z) errors in $|\psi\rangle_L$ are corrected. The states $|0\rangle_L$ and $|+\rangle_L$ should be prepared fault-tolerantly and free from erasure errors and the encoded SUM gate has pairwise implementation for CSS codes.

Implementation of error correction for erasure errors. Teleportation based error correction (TEC) [28, 29] has been shown to be an effective approach for the correction of erasure and operation errors for qubit encoding schemes. Since teleportation requires X and Z measurements on qubits, error correction for erasure and operation errors is possible if we can reliably measure the logical operators X_L and Z_L of the error correcting code [20]. For example, consider the logical operators of the $[[4, 1, 2]]$ code $X_L = IZIZ, ZIZI$ and $Z_L = IIXX, XXII$. If any qubit undergoes an erasure error, X_L and Z_L can still be expressed using the remaining three qubits, and consequently the encoded qubit can be retrieved.

TEC can be extended to multilevel systems [Fig. 2] by using generalized Pauli operators that act on d -level system as $X^l|j\rangle = |j+l\rangle$ and $Z^l|j\rangle = \omega^{(lj)}|j\rangle$, $0 \leq i, j \leq d-1$, $\omega^d = 1$ [30] and SUM gate that acts on a control qudit in state $|i\rangle$ with a target qudit in state $|j\rangle$ to produce the transformation $|i\rangle|j\rangle \rightarrow |i\rangle|(i+j) \bmod d\rangle$ [30]. The capability to measure X_L and Z_L is sufficient to correct erasure and operation errors using TEC. For example, consider the $[[3, 1, 2]]_3$ code with stabilizers XXX, ZZZ and logical operators $X_L = IXX^2, XX^2I, X^2IX$ and $Z_L = IZ^2Z, ZZ^2I, Z^2IZ$, it can be readily seen that in the presence of an erasure error on the particular qutrit one can measure the corresponding logical operators and reconstruct the encoded state.

An interesting alternative to TEC is provided by one-bit teleportation based error correction (OBTEC) [31] circuits, using which we can correct erasure errors. In OBTEC circuit, we carry out measurement only on the encoded block without the necessity of an encoded Bell pair. The advantage of considering OBTEC is that one can save half of the resources to perform error correction. However, in the presence of operation errors, one can consider TEC as it is fully fault-tolerant [20].

Application in quantum repeaters. One-way (or third generation) quantum repeaters [20, 21, 32] rely on quantum error correction to correct photon erasure errors from transmission and relay quantum information from one repeater station to the next. At each station, error

correction operations are performed before the message is transmitted to the next station. Since erasure errors are the most outstanding challenge for repeater schemes, it is important to consider quantum error correcting codes that can correct erasure errors very efficiently. Recently, it has been shown that quantum parity codes (QPC) [20, 21, 33] (a generalization of the $[[4, 1, 2]]$ code) can efficiently correct erasure and operation errors using TEC. Since QPyC can correct more erasure errors than QPC, it is reasonable to consider QPyC instead of QPC for one-way quantum repeaters, and expect a significant improvement for resource requirements and key generation rates.

For a systematic comparison of QPC and QPyC, we consider the conversion of a d -level qudit into $\log_2 d$ qubits and compare the performance of the codes by a cost coefficient $C'(L_{tot}) = \frac{2^{k+1} \lceil \log_2 d \rceil}{L_0 R}$ qubits \times km $^{-1}$ (bit/sec) $^{-1}$ where, L_{tot} is the total communication distance, L_0 is the repeater spacing, and R is the secure key generation rate. The $C'(L_{tot})$ refers to the number of qubits required per km for the generation of one secure bit in one second [20]. In Fig. 3(a), we compare the cost coefficients of QPyC and QPC for various L_{tot} . We find that in the absence of operation errors, the new scheme with QPyC and OBTEC can achieve a very small cost coefficient that is about 10 times less than for QPC with TEC for $L_{tot} = 10,000$ km. In Fig. 3(b), we study the dependence of $R \cdot t_0$, where t_0 is the time delay due to local quantum operations, with respect to the total distance of communication for small encoded blocks of QPyC, with spacing between the repeaters as 1 km and assuming absence of operation errors. It can be seen that for $t_0 = 1 \mu\text{s}$, $3(7)$ qudits are sufficient to reach 700(10,000) km with a key generation rates $R \approx 10(1000)$ kHz.

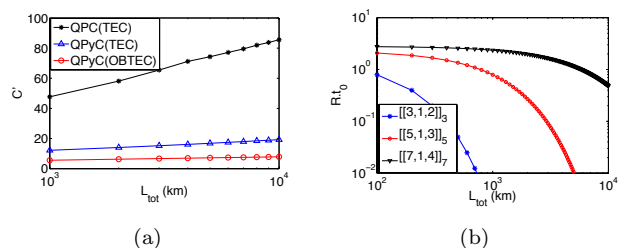


FIG. 3: (Color online) (a) A comparison of the cost coefficients of QPC (with TEC), QPC (with OBTEC) and QPyC (with OBTEC) in the absence of operation errors assuming that $t_0 = 1$ for small encoded blocks. (b) The key generation rates $R \cdot t_0$ that can be achieved with small blocks of QPyC in the absence of operation errors and with 1 km repeater spacing between the repeater stations.

Physical implementation. For the implementation of quantum repeaters with QPyC encoding schemes, it is advantageous to consider time-bin photonic qudits be-

cause they can be efficiently generated at telecom wavelengths and coupled into an optical fiber. A Controlled-Z (CZ) gate can be realized between two physical time-bin qudits by a generalization of the Duan-Kimble scheme [2] to multilevel systems. For qutrits, they can be realized in the recently demonstrated strong coupled neutral ^{87}Rb atom and micro-cavity system [34]. Multiple hyperfine energy levels, e.g. the transitions between $5^2\text{S}_{1/2}$, $F = 1$ and $5^2\text{P}_{3/2}$, $F = 1$ manifolds, can be considered. By controlling the Zeeman magnetic field, the transition frequencies relative to the cavity mode can be tuned precisely.

The procedure of Controlled-Z (CZ) gate between the time-bin qutrit (superposition of three pulses) and atom can be realized in three steps: 1. For the first incoming pulse, all energy levels are detuned from the cavity mode, then we have operation on atom energy levels as $U_{a,1} = \text{diag}\{1, 1, 1\}$. 2. For the second pulse, magnetic field is tuned so that the phase shift is $2\pi/3$, 0 and $-2\pi/3$, $U_{a,2} = \text{diag}\{e^{i\frac{2\pi}{3}}, 1, e^{-i\frac{2\pi}{3}}\}$. 3. For the third pulse, the magnetic field is reversed so that the phase shift is $-2\pi/3$, 0 and $2\pi/3$, then $U_{a,3} = \text{diag}\{e^{-i\frac{2\pi}{3}}, 1, e^{i\frac{2\pi}{3}}\}$.

One can implement a CZ gate between two time-bin photonic qutrits (f and s) by applying three photon-atom CZ gates ($C_{f,a} = \sum_m |m\rangle_f \langle m| \otimes U_{a,m}$ with $m = 1, 2, 3$ denoting the state of photon qutrits) and two Fourier gates (F_a) on atoms as [18] $U_{CZ} \rightarrow C_{f,a}^{-1} F_a^{-1} C_{s,a} F_a C_{f,a}$, if the atom is in an equal superposition of all energy levels where, $F_{j,k} = \frac{e^{[i \cdot (j-1) \cdot (k-1) \cdot 2\pi/3]}}{\sqrt{3}}$ for $j, k = 1, 2, 3$. The atom state initialization and Fourier gate of atom can be realized by the microwave or optical Raman pulsed controlled transitions ($|g_1\rangle \leftrightarrow |g_2\rangle$ and $|g_2\rangle \leftrightarrow |g_3\rangle$) and the phase gate Z . For $d \geq 3$, the CZ gate can be implemented by using the system of d atoms coupled to the same cavity mode. Each atom consists of a Λ transition, with ground states $|g\rangle$ and $|s\rangle$ and excited state $|e\rangle$. The $g - e$ transition is near resonance with the cavity mode, while the $s - e$ transition is far off-resonance. In addition, the transition frequencies of atoms can be controlled by external electric or magnetic field individually. To implement a CZ gate, the atoms are initialized to $|ss \dots s\rangle$, followed by single photon Raman transition to the one-excitation Dicke state $\frac{1}{\sqrt{d}}(|gs \dots s\rangle + |sg \dots s\rangle + \dots |ss \dots g\rangle)$. Then, the CZ gate of d -level time-bin qudit can be realized by precisely tuning the frequencies of atoms: for j -th ($j = 1, \dots, d$) pulse input to the system, the k -th ($k = 1, \dots, d$) atom are tuned to be near-resonance with the cavity so that the reflected pulse gain a phase of $e^{i\frac{\pi}{d}(j-1)(k-1)}$. The Fourier gate of atoms can be realized by virtual cavity photon mediated atom-atom interaction, with strong pumping on the $|s\rangle \leftrightarrow |e\rangle$ transition, with the frequency difference equals to the detuning between cavity photon and $|g\rangle \leftrightarrow |e\rangle$. Based on that, the CZ gate between two time-bin qudits can be realized with the same procedure

described earlier.

Summary and outlook. We investigated the usage of efficient codes of multilevel systems that can correct up to 50% erasure error rates to encode quantum information. The success probability of error correction of QPyC near 50% erasure rates is always higher than that of surface codes of all code sizes. We generalized TEC to multilevel systems and proposed its usage for the correction of erasure and operation errors, and a simpler resource efficient scheme - OBTEC to correct only erasure errors. In comparison with the earlier known one-way quantum repeater schemes that used QPC for encoding, we obtained a considerable improvement in resources for communication across 10,000km. In future, it will be interesting to consider the experimental implementation of multilevel systems using oscillators [35], Rydberg atoms [36] and ensembles of multilevel systems [37, 38]. Moreover, one can extend the coding schemes to continuous variables [39] for the correction of erasure errors. We can also consider the usefulness of quantum error correcting codes for multilevel systems that can correct a large fraction of erasure errors to improve precision metrology [40–42].

Acknowledgements This work was supported by the DARPA (Quiness program), ARO, ASFOR, MURI, NBRPC (973 program), the Packard Foundation and the Alfred P. Sloan Foundation. We thank Anup Rao, Hong Tang, Jungsang Kim, Mikhail Lukin, Norbert Lütkenhaus, Siddharth Prabhu and Steven Girvin for discussions.

* liang.jiang@yale.edu

- [1] E. Knill, R. Laflamme, and G. J. Milburn, Nature (London) **409**, 46 (2001).
- [2] L.-M. Duan and H. Kimble, Phys. Rev. Lett. **92**, 127902 (2004).
- [3] P. Kok, K. Nemoto, T. C. Ralph, J. P. Dowling, and G. J. Milburn, Rev. Mod. Phys. **79**, 135 (2007).
- [4] B. a. Bell, D. a. Herrera-Martí, M. S. Tame, D. Markham, W. J. Wadsworth, and J. G. Rarity, Nat. comm. **5**, 3658 (2014).
- [5] J. Vala, K. Whaley, and D. Weiss, Phys. Rev. A **72**, 052318 (2005).
- [6] J. Preskill, Proc. Natl. Acad. Sci. USA **454**, 385 (1998).
- [7] L.-a. Wu, M. Byrd, and D. Lidar, Phys. Rev. Lett. **89**, 127901 (2002).
- [8] R. Fazio, G. Palma, and J. Siewert, Phys. Rev. Lett. **83**, 5385 (1999).
- [9] D. L. Moehring, P. Maunz, S. Olmschenk, K. C. Younge, D. N. Matsukevich, L.-M. Duan, and C. Monroe, Nature **449**, 68 (2007).
- [10] S. Ritter, C. Nölleke, C. Hahn, A. Reiserer, A. Neuzner, M. Uphoff, M. Mücke, E. Figueroa, J. Bochmann, and G. Rempe, Nature **484**, 195 (2012).
- [11] H. Bernien, B. Hensen, W. Pfaff, G. Koolstra, M. S. Blok, L. Robledo, T. H. Taminiau, M. Markham, D. J. Twitchen, L. Childress, and R. Hanson, Nature **497**, 86

- (2013).
- [12] C. Monroe, R. Raussendorf, A. Ruthven, K. R. Brown, P. Maunz, L.-M. Duan, and J. Kim, *Phys. Rev. A* **89**, 022317 (2014).
- [13] M. Varnava, D. Browne, and T. Rudolph, *Phys. Rev. Lett.* **97**, 120501 (2006).
- [14] S. D. Barrett and T. M. Stace, *Phys. Rev. Lett.* **105**, 200502 (2010).
- [15] T. M. Stace and S. D. Barrett, *Phys. Rev. A* **81**, 022317 (2010).
- [16] R. Gingrich, P. Kok, H. Lee, F. Vatan, and J. Dowling, *Phys. Rev. Lett.* **91**, 217901 (2003).
- [17] C. H. Bennett, D. P. DiVincenzo, and J. a. Smolin, *Phys. Rev. Lett.* **78**, 3217 (1997).
- [18] D. Aharonov and M. Ben-or, *SIAM J. Comput.* **38**, 1207 (2008).
- [19] R. Cleve, D. Gottesman, and H.-K. Lo, *Phys. Rev. Lett.* **83**, 648 (1999).
- [20] S. Muralidharan, J. Kim, N. Lütkenhaus, M. D. Lukin, and L. Jiang, *Phys. Rev. Lett.* **250501**, 1 (2014).
- [21] W. J. Munro, a. M. Stephens, S. J. Devitt, K. a. Harrison, and K. Nemoto, *Nat. Photonics* **6**, 777 (2012).
- [22] C.-Y. Lu, W.-B. Gao, J. Zhang, X.-Q. Zhou, T. Yang, and J.-W. Pan, *Proc. Natl. Acad. Sci. USA* **105**, 11050 (2008).
- [23] See Supplementary Material for OBTEC, critical exponents and error model and key generation rates. .
- [24] M. Grassl, T. Beth, and T. Pellizzari, *Phys. Rev. A* **56**, 33 (1997).
- [25] A. G. Fowler, M. Mariantoni, J. M. Martinis, and A. N. Cleland, *Physical Review A* **86**, 032324 (2012).
- [26] R. Langlands, P. Pouliot, and Y. Saint-Aubin, arXiv preprint math/9401222 **30** (1994).
- [27] R. Langlands, P. Pouliot, and Y. Saint-Aubin, *Bulletin of the American Mathematical Society* **30**, 1 (1994).
- [28] E. Knill, *Phys. Rev. A* **71**, 042322 (2005).
- [29] E. Knill, *Nature (London)* **434**, 39 (2005).
- [30] D. Gottesman, *Quantum Computing and Quantum Communications* **1509**, 302 (1999).
- [31] X. Zhou, D. Leung, and I. Chuang, *Phys. Rev. A* **62**, 052316 (2000).
- [32] A. G. Fowler, D. S. Wang, C. D. Hill, T. D. Ladd, R. Van Meter, and L. C. L. Hollenberg, *Phys. Rev. Lett.* **104**, 180503 (2010).
- [33] T. Ralph, A. Hayes, and A. Gilchrist, *Phys. Rev. Lett.* **95**, 100501 (2005).
- [34] J. D. Thompson, T. G. Tiecke, N. P. de Leon, J. Feist, a. V. Akimov, M. Gullans, a. S. Zibrov, V. Vuletić, and M. D. Lukin, *Science* **340**, 1202 (2013).
- [35] V. V. Albert, S. Krastanov, C. Shen, R.-B. Liu, R. J. Schoelkopf, M. H. Devoret, M. Mirrahimi, and L. Jiang, [quantph:/1503.00194](https://arxiv.org/abs/1503.00194), 5 (2015), arXiv:1503.00194 .
- [36] A. Rauschenbeutel, G. Nogues, and S. Osnaghi, *Science* **288**, 2024 (2000).
- [37] E. Brion, K. Mølmer, and M. Saffman, *Phys. Rev. Lett.* **99**, 260501 (2007).
- [38] E. Brion, L. Pedersen, M. Saffman, and K. Mølmer, *Phys. Rev. Lett.* **100**, 110506 (2008).
- [39] S. Krastanov, V. V. Albert, C. Shen, C.-L. Zou, R. W. Heeres, B. Vlastakis, R. J. Schoelkopf, and L. Jiang, , 5 (2015), arXiv:1502.08015 .
- [40] E. M. Kessler, I. Lovchinsky, a. O. Sushkov, and M. D. Lukin, *Phys. Rev. Lett.* **112**, 150802 (2014).
- [41] G. Arrad, Y. Vinkler, D. Aharonov, and A. Retzker, *Phys. Rev. Lett.* **112**, 150801 (2014).
- [42] W. Dür, M. Skotiniotis, F. Fröwis, and B. Kraus, *Phys. Rev. Lett.* **112**, 080801 (2014).
- [43] L. Sheridan and V. Scarani, *Phys. Rev. A* **82**, 030301 (2010).

Supplementary information on: Overcoming erasure errors in quantum memories with multilevel systems

Let us consider the following encoding procedure which maps an unknown single qubit into a quantum error correcting code through $\alpha|0\rangle + \beta|1\rangle \rightarrow \alpha|0\rangle_L + \beta|1\rangle_L$, where each physical qubit is mapped into two Bell states as follows [22],

$$\begin{aligned} |0\rangle_L &= \frac{1}{2}(|00\rangle + |11\rangle)_{12}(|00\rangle + |11\rangle)_{34}, \\ |1\rangle_L &= \frac{1}{2}(|00\rangle - |11\rangle)_{12}(|00\rangle - |11\rangle)_{34}, \end{aligned} \quad (7)$$

where the subscripts 1-4 denote qubits 1-4. Suppose now we transmit this encoded qubit through a channel and it undergoes at most one erasure error. The quantum error correcting codes enable the reconstruction of the encoded qubit as follows. First, the location of the lost photon can be detected by a quantum non-demolition measurement. Next, to reconstruct the encoded qubit we need to measure its complementary qubit in the Z-basis with the measurement outcome $a \in \{0, 1\}$. That is, if qubit 1 is lost we measure qubit 2; or if qubit 3 is lost we measure qubit 4. Suppose qubit 1 is lost, after measuring qubit 2, the state of the system collapses to a pure state $\alpha(|00\rangle + |11\rangle)_{34} + (-1)^a\beta(|00\rangle - |11\rangle)_{34}$. As such, the original state $\alpha|0\rangle + \beta|1\rangle$ is recovered as we know the value of a . Note that here; in order to encode a physical qubit into an encoded state, one needs at least four qubits to correct one arbitrary erasure error.

To reduce the consumption of the resources, one possibility is to explore multi-level systems. As shall be shown below, it is feasible to correct an arbitrary erasure error with a quantum code of just *three qutrits* instead of four qubits. As an example, let us consider the following code which encodes a qutrit $\alpha|0\rangle + \beta|1\rangle + \gamma|2\rangle$ into three qutrits [19],

$$\begin{aligned} |0\rangle_L &= \frac{1}{\sqrt{3}}(|000\rangle + |111\rangle + |222\rangle)_{123} \\ |1\rangle_L &= \frac{1}{\sqrt{3}}(|012\rangle + |120\rangle + |201\rangle)_{123}. \\ |2\rangle_L &= \frac{1}{\sqrt{3}}(|021\rangle + |210\rangle + |102\rangle)_{123}. \end{aligned} \quad (8)$$

Here, the subscripts 1-3 represent qutrits 1-3. Suppose, a single qutrit is lost, then it is possible to reconstruct the secret using qutrits 1 and 2. For example, if qutrit 1 is lost, then the state of qutrits 2 and 3 are given by,

$$\rho_{23} = \sum_{i=0}^2 |\psi_i\rangle_{23}\langle\psi_i| \quad (10)$$

where,

$$\begin{aligned} |\psi_0\rangle &= \alpha|00\rangle_{23} + \beta|12\rangle_{23} + \gamma|21\rangle_{23} \\ |\psi_1\rangle &= \alpha|11\rangle_{23} + \beta|20\rangle_{23} + \gamma|02\rangle_{23} \\ |\psi_2\rangle &= \alpha|22\rangle_{23} + \beta|01\rangle_{23} + \gamma|10\rangle_{23}. \end{aligned} \quad (11)$$

We now apply the circuit shown in Fig. 4 to $|\psi_i\rangle$ to obtain the encoded state $\alpha|0\rangle + \beta|1\rangle + \gamma|2\rangle$.

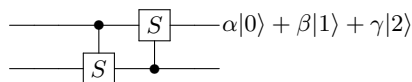


FIG. 4: The circuit used to decode the encoded qutrit.

One can also reconstruct the encoded qutrit using the OBTEC circuit as shown in Fig. 5. OBTEC can be extended to higher number of qudits in a similar fashion.

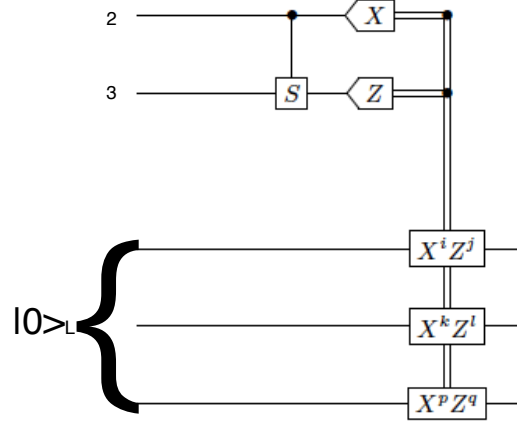


FIG. 5: OBTEC circuit for the $[[3, 1, 2]]_3$ code

Note that the four-qubit code and the three-qutrit code only work for a single erasure error. In practice, we will experience more photon erasures and therefore, we need quantum error correcting codes that are capable of correcting more than one erasure error. Interestingly, both quantum error-correcting codes of qudits and qutrits can be generalized for more erasure errors. Specifically, the four-qubit code can be generalized to (n, m) quantum parity codes [33] by encoding each qubit into an n GHZ states of length- m each. This code works efficiently only for small erasure errors ($\approx 20\%$). The second code with qutrits can be generalized to $[[2k + 1, 1, k + 1]]_d$ QPyC of qudits which can correct up to 50% erasure errors that are considered in the Letter.

CRITICAL EXPONENTS

The success probability for the QpyC $[[2k + 1, 1, k + 1]]_k$ is

$$P_{success}(k, p_l) = \sum_{i=0}^k \binom{2k+1}{i} (p_l)^i (1-p_l)^{2k+1-i} \quad (12)$$

$$= 1 - \binom{2k+1}{k+1} (p_l)^{k+1} (1-p_l)^k {}_2F_1\left(1, -k; k+2; \frac{-p_l}{1-p_l}\right), \quad (13)$$

where ${}_2F_1(a, b; c; d)$ is the Hypergeometric function. Around the fixed point $P_{success}(k, \frac{1}{2}) = \frac{1}{2}$, the asymptotic expression is

$$P_{success}(k, p_l) = 1 - A - (2A + B)(p_l - \frac{1}{2}) + o[(\frac{1}{2} - p_l)^2]. \quad (14)$$

where $A = \binom{2k+1}{k} 2^{-2k-2} \frac{\sqrt{\pi}\Gamma(k+2)}{\Gamma(k+3/2)}$ and $B = \binom{2k+1}{k} 2^{-2k+1} \frac{k \times {}_2F_1(2, 1-k; k+3; -1)}{k+2}$. For $k \rightarrow \infty$, make the approximation that $\binom{2k+1}{k} \approx \sqrt{\frac{1}{k\pi}} 2^{2k+1}$, $\frac{\Gamma(k+2)}{\Gamma(k+3/2)} \approx \sqrt{k}$ and $\frac{{}_2F_1(2, 1-k; k+3; -1)}{k+2} \approx \frac{1}{2}$, then $A \approx \frac{1}{2}$ and $B \approx 2\sqrt{\frac{k}{\pi}}$, thus

$$P_{success}(k, p_l) = \frac{1}{2} - (1 + 2\sqrt{\frac{k}{\pi}})(p_l - \frac{1}{2}) + o[(\frac{1}{2} - p_l)^2]. \quad (15)$$

$$\approx \frac{1}{2} - 2\sqrt{\frac{k}{\pi}}(p_l - \frac{1}{2}) \quad (16)$$

for $k \gg 1$. That means for given $P_{success}$, we need the QpyC with the size

$$k \approx \frac{\pi}{4} \left(\frac{P_{success} - \frac{1}{2}}{\frac{1}{2} - p_l} \right)^2. \quad (17)$$

ERROR MODEL AND KEY GENERATION RATES

In this section, we will consider various possible operation errors acting on the encoded qubit as it propagates from the sender to the receiver through many repeater stations. Suppose that each physical qudit is encoded into a $[[2k + 1, 1, k + 1]]_d$ QPYC and is transmitted to its neighboring repeater station, where the TEC is implemented. In our quantum-repeater design, each station is equipped with TEC circuit to correct both the X^i or Z^j errors. We assume independent errors acting on physical qubits for the sake of simplicity. We consider an extensive error model with the following types of errors acting on the encoded qubit as follows:

1. The photon arrives at each repeater station with probability $1 - p_l = e^{-\frac{L_0}{L_{att}}}$, where L_0 is the repeater spacing and L_{att} is the attenuation length of the fiber.
2. The photon undergoes depolarization with a probability ϵ_d , which also coincides with the probability of error on each physical qubit of the encoded Bell pair prepared at the repeater station.
3. The photon experiences an additional dephasing in the matter qubit-photon coupling with a probability ϵ_p .
4. Each SUM gate acting between the encoded Bell pair and the incoming qubit (see Fig. 2) fails at a probability ϵ_g .

By further assuming same probabilities for all types of depolarization errors and gate errors, the transmission channel ρ_{RS} with the incoming state R and the state S at the repeater station takes the form,

$$E_c(\rho_R) = (1 - p_l)(1 - \epsilon_d - \epsilon_p) + p_l|vac\rangle\langle vac| + \frac{(1 - p_l)\epsilon_d}{d^2} \sum_{i,j=0}^{d-1} (X^i Z^j) \rho_R (X^i Z^j)^\dagger + \frac{(1 - p_l)\epsilon_p}{d} \sum_{p=0}^{d-1} (Z^p) \rho (Z^p)^\dagger. \quad (18)$$

Similarly, the gate error can be modeled as

$$E_g(\rho_{RS}) = (1 - \epsilon_g) U_{sum} \rho_{RS} U_{sum}^\dagger + \frac{\epsilon_g}{d^4} \sum_{a=0}^{d-1} \sum_{b=0}^{d-1} \sum_{c=0}^{d-1} \sum_{d=0}^{d-1} (X^a Z^b X^c Z^d) \rho_{RS} (X^a Z^b X^c Z^d)^\dagger. \quad (19)$$

For each qudit the locally prepared logical states $|0\rangle_L$ and $|+\rangle_L$ are modelled as

$$E_p(\rho_S) = (1 - \epsilon_d) \rho_S + \frac{\epsilon_d}{d^2} \sum_{i,j=0}^{d-1} (X^i Z^j) \rho_S (X^i Z^j)^\dagger. \quad (20)$$

From these error channels, we can calculate the probability of having an error in any one of the measurements as

$$\begin{aligned} \epsilon_X &= \frac{\epsilon_g}{d^4} (d^4 - d^3) + \frac{2\epsilon_d}{d^2} (d^2 - d) \\ \epsilon_Z &= \frac{\epsilon_g}{d^4} (d^4 - d^3) + \frac{2\epsilon_d}{d^2} (d^2 - d) + \frac{\epsilon_p}{d} (d - 1). \end{aligned} \quad (21)$$

Once the encoded state $[[2k + 1, 1, k + 1]]_d$ is transmitted from one repeater station to its neighbor, there exists three possibilities at the receiving repeater station

1. More than k photons are lost in transit and the outcome of the measurement cannot be found leading to a heralded failure with probability p_{fail} .
2. At least k photons are received, but the encoded state is not decoded correctly due to the presence of the presence of many operation errors and the encoded state is not decoded correctly with probability $p_{incorrect}$.
3. At least k photons are received to make an encoded X/Z measurement and the encoded state is decoded correctly with probability $p_{correct}$.

The probability that more than k photons are lost during transit is

$$p_{fail} = \sum_{n_1=k+1}^{2k+1} \binom{2k+1}{n_1} p_l^{n_1} (1-p_l)^{2k+1-n_1} \quad (22)$$

The probability that a heralded failure does not happen at any one of the R repeater stations is given by,

$$P_{succ}(R) = (1 - p_{fail})^R. \quad (23)$$

Let us suppose that n_1 photons are lost before the destination. Among the rest of the $(2k+1-n_1)$ photons that arrive the destination, n_2 photons suffer operation errors. As such, the code can correct up to $n_1 + 2n_2 \leq k$ errors. The probability of successfully measuring the encoded X/Z measurement outcomes is given by,

$$p_{correct(X/Z)} = \sum_{n_1=0}^k \sum_{n_2=0}^{\lfloor \frac{k}{2} - \frac{n_1}{2} \rfloor} \binom{2k+1}{n_1} \binom{2k+1-n_1}{n_2} (p_l)^{n_1} \epsilon_{X/Z}^{n_2} (1-p_l)^{2k+1-n_1} (1-\epsilon_{X/Z})^{2k+1-n_1-n_2} \quad (24)$$

The probability of incorrect decoding of the qudit is given by,

$$p_{incorrect(X/Z)} = \sum_{n_1=0}^k \sum_{n_2=\lceil \frac{k}{2} - \frac{n_1}{2} + \frac{1}{2} \rceil}^{2k+1-n_1} \binom{2k+1}{n_1} \binom{2k+1-n_1}{n_2} p_l^{n_1} \epsilon_{X/Z}^{n_2} (1-p_l)^{2k+1-n_1} (1-\epsilon_{X/Z})^{2k+1-n_1-n_2} \quad (25)$$

It is easy to verify that $p_{fail(X/Z)} + p_{correct(X/Z)} + p_{incorrect(X/Z)} = 1$. The fidelity of the encoded quantum information can be defined as,

$$F_{X/Z} = \frac{[p_{correct(X/Z)}]^R}{P_{succ}(R)}. \quad (26)$$

For the two state protocol for quantum key distribution (where information is encoded in only two logical bases X^1 and Z^1), the asymptotic normalized key generation rate is [43].

$$R = \frac{P_{success}}{t_0} (\log_2 d - 2h(Q)), \quad (27)$$

with

$$\begin{aligned} Q &= 1 - \left(\frac{F_X + F_Z}{2} \right) \\ h(Q) &= -Q \log_2 \frac{Q}{d-1} - (1-Q) \log_2 (1-Q). \end{aligned} \quad (28)$$

The variation of optimized $C'(L_{tot})$ is shown in Fig. 6.

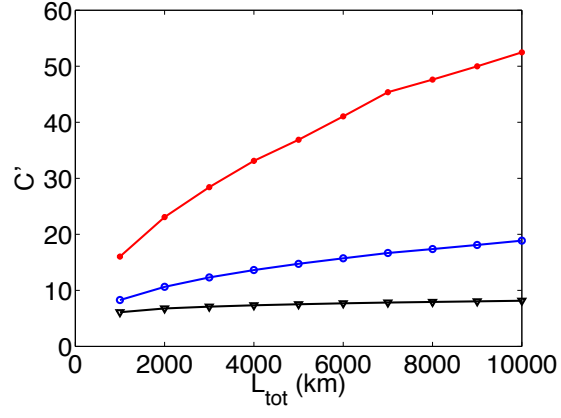


FIG. 6: Optimized cost coefficient C' of QPyC with TEC in the presence of operation errors. The red curve corresponds to $\epsilon_d = 10^{-3}d^2$, $\epsilon_g = 10^{-3}d^4$, $\epsilon_p = 10^{-3}d$, the blue curve corresponds to $\epsilon_d = 10^{-4}d^2$, $\epsilon_g = 10^{-4}d^4$, $\epsilon_p = 10^{-4}d$, the black curve corresponds to $\epsilon_d = 10^{-4}d^2$, $\epsilon_g = 10^{-6}d^4$, $\epsilon_p = 10^{-4}d$